

# Design Analysis and Modeling of a General Aviation Aircraft

F. H. Darwish<sup>a,\*</sup>, G. M. Atmeh<sup>b</sup>, Z. F. Hasan<sup>c</sup>

<sup>a</sup>Aeronautical Engineering Dept., Faculty of Engineering, Jordan University of Science and Technology, Irbid 22110, Jordan

<sup>b</sup>Mechanical and Aerospace Engineering Dept., University of Texas at Arlington, Arlington, Texas

<sup>c</sup>Mechanical Engineering Dept., Texas A&M University, College Station, Texas

## Abstract

In the present study, design analysis is performed to accurately estimate the gross take-off weight, define the external geometry, and size the wings and tail of a general aviation aircraft by using the performance parameters associated with a pre-defined mission profile and a set of design goals. Three-dimensional layout and projections of the design airplane are created using conic lofting-based software. The airplane configuration, the estimated weight, and the real time airplane equations of motion are then introduced to a simulation environment in Matlab to visualize the take-off, climb and cruise segments of the mission profile. The simulation has proven the adherence of the design analysis and its results to the design goals. In addition, finite element software package COMSOL is implemented to perform static stress analysis on the selected wing configuration when subjected to the generated aerodynamic loads to examine its structural reliability. The finite element results have shown that the selected wing configuration is a safe candidate for the present general aviation airplane implementation.

© 2012 Jordan Journal of Mechanical and Industrial Engineering. All rights reserved

Keywords: Aircraft Design; Flight Simulation; Finite Element Analysis

Nomenclature			
$a$	airfoil lift slope	$M_z$	bending moment around the z-axis
$A_b$	boom area	$P$	power
$A_n$	Fourier coefficient	$q$	shear flow
$AR$	aspect ratio	$Q$	pitching rate
$b$	span	$S$	plan form area of the wing
$c$	chord length	$S_{HT}$	plan form area of the horizontal tail
$\bar{c}$	mean aerodynamic chord	$S_{VT}$	plan form area of the vertical tail
$c_d$	drag coefficient per unit span	$S_x$	shear force in the x-axis
$c_{do}$	zero-lift drag coefficient per unit span	$S_z$	shear force in the z-axis
$c_l$	lift coefficient per unit span	$u$	linear velocity in the x-direction
$c_m$	pitching moment coefficient per unit span	$V_\infty$	free stream velocity
$c_r$	chord length at the root	$w$	linear velocity in the z-direction
$c_t$	chord length at the tip	$W$	instantaneous weight of the aircraft
$C_{HT}$	volume coefficient of the horizontal tail	$W_c$	weight of the crew
$C_{VT}$	volume coefficient of the vertical tail	$W_e$	empty weight of the aircraft
$D'$	drag force per unit span	$W_f$	weight of the fuel
$D_{f,max}$	maximum diameter of the fuselage	$W_o$	gross take-off weight of the aircraft
$F$	external force	$W_p$	weight of the payload
$g$	constant of gravity	$X_B$	body x-axis
$I_{m,yv}$	mass moment of inertia around the y-axis	$X_I$	inertial x-axis
$I_{xx}$	second moment of area around the x-axis	$y$	span-wise distance
$I_{zz}$	second moment of area around the z-axis	$Y$	general y-axis
$I_{xz}$	product moment of area	$\bar{Y}$	distance of the mean aerodynamic chord
$k$	induced drag coefficient	$Z_B$	body z-axis
$L'$	lift force per unit span	$Z_I$	inertial z-axis
$L_f$	length of the fuselage	$\alpha_O$	zero-lift angle of attack
$L_{HT}$	distance between the horizontal tail and the wing	$\alpha_G$	geometric angle of attack
$L_{VT}$	distance between the vertical tail and the wing	$F$	fineness ratio
$m$	mass of the aircraft	$G$	vortex strength
$M$	pitching moment	$l$	taper ratio
$M_x$	bending moment around the x-axis	$q$	pitching angle
		$r$	air density
		$s$	direct stress
		$y$	angle of twist

\* Corresponding author. e-mail: fhdarwish@just.edu.jo

## 1. Introduction

The design of an aircraft is a prolonged process that consists mainly of three design phases which are: the conceptual design, the preliminary design, and the detailed design. The phase of conceptual design, which is the umbrella of the present research, deals mainly with developing a layout of the aircraft's external geometry, major systems and components; and determining the gross weight and the performance characteristics that the airplane must have in order to achieve its design goals.

The area of structural analysis and modeling of major aircraft components and its relevance to the conceptual design of aircrafts has attracted researchers and structural engineers in the aircraft industry. Giles [1] introduced a design-oriented analysis capability for aircraft fuselage structure. The new analysis capability and an existing wing analysis procedure were combined to model the entire airframe. Saha et al [2] presented a design analysis study of a hypothetical lightweight combat aircraft through thermodynamical, aerodynamical, and performance considerations of predefined mission requirements. The authors concluded that their design has fulfilled the numerous mandatory requirements demanded for an interceptor aircraft. A flexible approach for multidisciplinary design analysis and optimization, and its application to aircraft wing design was presented by Kessler and Vankan [3]. Their results have shown significant improvements of the wing performance for different design goals which in turns approved the effectiveness and flexibility of the proposed approach. Tarkian and Zaldivar Tessier [4] introduced a frame work which enables a holistic view of the aircraft systems through a multidisciplinary analysis approach. The connection between the tools for aerodynamic analysis and CAD modeling were made fully automatic. This approach put the designers one-step closer to a non-statistical holistic approach for aircraft conceptual design. A detailed structural and stress analysis on an aerodynamically loaded Cessna aircraft wing were performed by Al-Mawahra and Zaza [5]. They investigated the structural effectiveness of the wing constructing components when subjected to the various aerodynamic loads.

The main objective of the present paper is to introduce an environment for a real time simulation of the aircraft motion based on the specifications of the flight mission profile; performance parameters, the geometry and the weight of the airplane to verify the adherence of the conceptual design geometric product to the initial design requirements. In addition, the structural capability of the selected wing and sub components to withstand the generated aerodynamic loads is examined through finite element modeling and analysis using the finite element software package COMSOL [6].

## 2. The Conceptual Design

### 2.1. Design approach:

As described in reference [7], a set of design goals or requirements along with a flight mission profile must be available to provide a baseline for the conceptual design

process. Initially, a crude method of weight estimation based on an initial sketch of how the airplane is envisioned is conducted to achieve an initial estimate of the weight of the airplane. This step is not linked to any other steps of the design procedure. It is basically performed to obtain an initial estimate of the airplane weight that can be used later for comparison with the final weight estimation to validate the results. In order to obtain an accurate estimate of the airplane weight, the performance parameters; wing loading (W/S), and the power-to-weight ratio (P/W) must be first calculated for each segment of the flight mission profile. Subsequently, the minimum wing loading and the maximum power-to-weight ratio are selected in order to satisfy the performance requirements of the entire flight and to be used later in the gross weight calculation. The major dimensions of the external geometry of the aircraft such as the fuselage length and diameter; the wing span and plan form area; and the tail specifications can be obtained by using of the selected performance parameters and the estimated weight as will be shown in the following sections. Finally, the method of conic lofting is used to generate a three-dimensional layout of the airplane by using the RDS software of reference [7].

### 2.2. Design goals:

The conceptual design is commenced by defining a set of design goals. Based on the existing data of many different general aviation airplanes, the design goals of the present airplane are set as follows:

- Single engine airplane with a maximum velocity > 76 m/s.
- Stall velocity = 18 m/s
- Take-off ground roll distance < 305 m
- Landing distance < 427 m
- Range = 1000 km
- Service ceiling = 3962 m
- Maximum rate of climb = 6 m/s

This set of design goals is considered as a baseline for the conceptual design process.

### 2.3. Mission profile and initial sketch:

A simple mission profile that consists of five segments which are the take-off, climb, cruise, loiter and landing is considered for the present design analysis and is shown in figure 1.

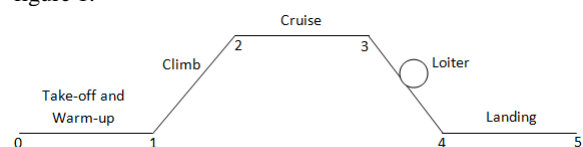


Figure 1: Mission profile.

Figure 2 shows the initial hand sketch of the aircraft. This basic sketch tentatively specifies the vertical location and geometry of the wings, the type and location of the tail, the landing gear, the engine and the cockpit locations.

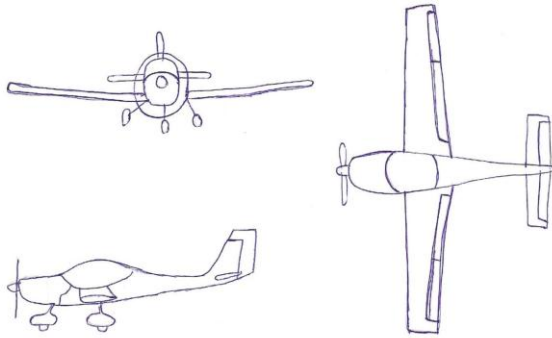


Figure 2: Initial sketch.

#### 2.4. Weight estimation based on an initial sketch:

The airplane gross take-off weight is basically the sum of the weight of the crew, the weight of the payload, the weight of the fuel, and the empty weight of the airplane.

$$W_o = W_c + W_p + W_f + W_e \quad (1)$$

The terms of equation (1) are rearranged and the take-off gross weight is expressed in terms of the crew and payload weight; the fuel weight fraction and the empty weight fraction as in equation (2), [7].

$$W_o = \frac{W_c + W_p}{1 - (W_f/W_o) - (W_e/W_o)} \quad (2)$$

The crew and payload weights are normally prescribed in the design requirements. The fuel weight fraction primarily depends on the amounts of fuel burned during each segment of the mission profile or, in other words, on the weight fraction across each segment of the mission profile. The empty weight fraction however is unknown and is statistically a function of the take-off gross weight as in equation (3), [7].

$$\frac{W_e}{W_o} = AW_o^C \quad (3)$$

The parameters A and C in the above equation are statistical constants that depend on the shape of the airplane which is tentatively shown in the sketch of figure 2, and on the family of the airplane, for example, general aviation in the present study. Accordingly, the calculation of the gross weight through equation (2) is an iterative process that starts with an initial guess of the gross take-off weight. Based on this method, the crude estimate of the airplane gross weight is found to be 757.5 Kg. More details about the calculation of the fuel weight fraction and the empty weight fraction are provided in reference [7].

#### 2.5. Weight estimation based on the performance parameters:

This method is more sophisticated than the one presented in the previous section and provides a better estimation of the gross weight of the airplane as the performance parameters are integrated in the gross weight equation. The difference between the two methods is basically in the calculation of the empty weight fraction. In

this method the empty weight fraction is function of the wing loading, power-to-weight ratio, the wing aspect ratio (AR), the maximum cruising velocity, and the airplane gross weight as presented in equation (4), [7].

$$W_e/W_o = a + bW_o^{C1} AR^{C2} (W/S)^{C3} (P/W)^{C4} V_{max}^{C5} \quad (4)$$

Where a, b, C1, C2, C3, C4, and C5 are statistical constants that depend on the family of the airplane [7]. In the above equation, the wing loading and the power-to-weight ratio are the minimum and the maximum respectively, of all segments of the mission profile. Some equations that are used to calculate the wing loading and the power-to-weight ratio are mathematically interconnected which makes the analysis lengthy and complicated. In addition, some geometric and aerodynamic parameters such as the wing aspect ratio, taper ratio, airfoil type and characteristics, and the drag coefficient are needed for the analysis to prepare equation (4). These parameters are not prescribed in the design requirements but can be carefully selected to serve achieving the design goals. Table 1 lists all the selected parameters, their values, and the resulting minimum wing loading and maximum power-to-weight ratio.

Table 1: Minimum wing loading and maximum power-to-weight ratios along with the required geometric and aerodynamic parameters needed for their calculations.

Required Aerodynamic and Geometric Parameters	
Wing root airfoil	NACA 23018
Wing tip airfoil	NACA 23012
Wing maximum lift coefficient	2.34
Maximum lift-to-drag ratio	12.9
Oswald efficiency factor	0.8
Zero-lift drag coefficient	0.03
Taper ratio	0.5
Aspect ratio	8
Fuselage fineness ratio	5.5
Calculated Wing Loading and Power-to-Weight Ratio	
Minimum wing loading	78.1 Kg/m <sup>2</sup>
Maximum power-to-weight ratio	0.15 hp/Kg

Now that the required performance parameters are available the gross-takeoff weight can be iteratively calculated by invoking equation (4) into equation (2). The converging solution of the gross weight of the airplane was found to be 952.5 Kg.

#### 2.6. Geometry sizing:

The geometry of a trapezoidal wing can now be unveiled after having the gross weight of the airplane, the wing loading, the wing aspect ratio and taper ratio. The following equations can be used to calculate the wing plan form area, the wing span, the root chord, the tip chord, the length and the location of the aerodynamic chord respectively.

$$S = \frac{W_o}{(W/S)} \quad (5)$$

$$b = \sqrt{AR.S} \quad (6)$$

$$c_r = \frac{2S}{b(1+\lambda)} \quad (7)$$

$$c_t = c_r \cdot \lambda \quad (8)$$

$$\bar{c} = \frac{(2/3)c_r(1+\lambda+\lambda^2)}{(1+\lambda)} \quad (9)$$

$$\bar{Y} = (b/6) \frac{(1+2\lambda)}{1+\lambda} \quad (10)$$

The fuselage main dimensions which are the length and maximum diameter can also be determined having available the airplane gross weight and the fineness ratio which represents the ratio between the fuselage length and maximum diameter. The length of the fuselage is related to the gross weight of the airplane and the statistical constants  $m$  and  $n$  as shown in equation (11), [7]. Subsequently, the maximum diameter can then be calculated from equation (12).

$$L_f = mW_o^n \quad (11)$$

$$\phi = \frac{L_f}{D_{f,max}} \quad (12)$$

The results of equations 5 to 12 are presented in table 2.

Table 2: Wing and fuselage dimensions.

Wing area	12.2 m <sup>2</sup>
Wing span	9.9 m
Wing root chord	1.65 m
Wing tip chord	0.8 m
Wing mean aerodynamic cord	1.3 m
Mean aerodynamic cord location along span	2.19 m
Fuselage length	7.7 m
Fuselage maximum diameter	1.4 m

The wing geometry and dimensions are shown in figure 3.

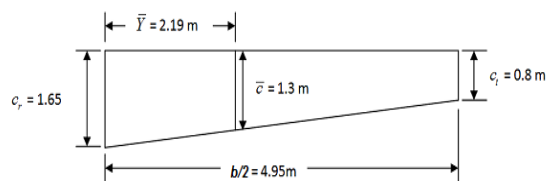


Figure 3: Wing geometry and dimensions.

The vertical and horizontal trapezoidal tails of the airplane are sized in a similar manner, however; depending on the volume coefficients of the vertical tail and the horizontal tail which express the effectiveness of the tail moments coefficients. Values of the horizontal and vertical tail coefficients vary according to the mission category of the aircraft [7]. The equations below allow for the calculation of the vertical and horizontal tail areas respectively.

$$S_{VT} = \frac{C_{VT} b S}{L_{VT}} \quad (13)$$

$$S_{HT} = \frac{C_{HT} \bar{c} S}{L_{HT}} \quad (14)$$

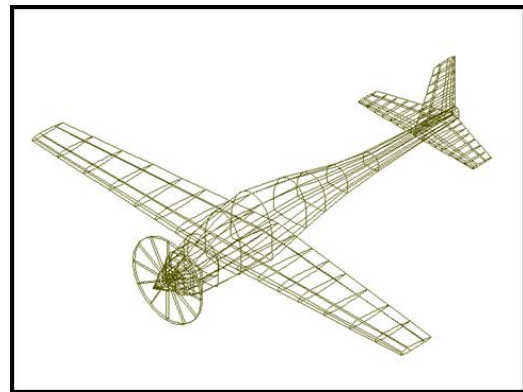
Accordingly, the plan form area, the span, the root and tip chords of the vertical and horizontal trapezoidal tails are found and summarized in table 3.

Table 3: Horizontal and vertical tails dimensions.

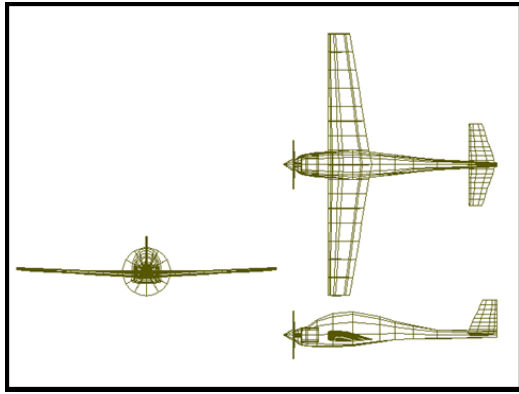
Horizontal Tail	
Span	3 m
Root cord	1 m
Tip cord	0.56 m
Mean aerodynamic cord	0.81 m
Mean aerodynamic cord location along span	0.68 m
Vertical Tail	
Span	1.2 m
Root cord	1.1 m
Tip cord	0.55 m
Mean aerodynamic cord	0.85 m
Mean aerodynamic cord location along span	0.27 m

## 2.7. Design layout:

As introduced, the main objective of the conceptual design is to provide lay-out drawings of the design airplane that feature its external geometry which has to be in general producible, aerodynamically smooth and credible. Conic lofting is a technique which incorporates a family of second degree curves to define the external geometry of airplanes and ships as well. In this study, the conic lofting technique is used to generate drawings of the designed airplane using the RDS software. Figures 4a and 4b show an isometric and three-view layout respectively of the airplane developed in RDS.



4a



4b

Figure 4: a) Aircraft isometric layout, b) Aircraft three-view layout.

### 3. Takeoff Simulation

The next step after defining the external geometry of the airplane is to create a three-dimensional model using the V-realm Builder software [8] and place it in a simulation environment, as shown in figure 5, by incorporating Matlab's simulink [9].

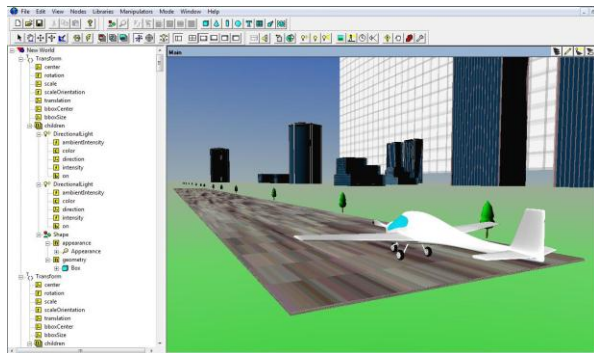


Figure 5: Simulation environment and three-dimensional model.

The intention of the simulation is to prove the ability of the design airplane to satisfy the predefined design goals. The simulation has considered three-degree-of-freedom motion of the airplane which includes the translation in the XI and ZI inertial directions and rotation in XI -ZI plane (perpendicular to the Y axis) as shown in figure 6. Equations 15, 16, and 17 represent the general governing equations of the airplane motion and are solved to obtain the displacement, velocity and acceleration in the body frame (XB -ZB) as functions of time.

$$\dot{u} = \frac{F_x}{m} - Qw - g \sin(\theta) \quad (15)$$

$$\dot{w} = \frac{F_z}{m} + Qu + g \cos(\theta) \quad (16)$$

$$\dot{Q} = \frac{M}{I_{m,yy}} \quad (17)$$

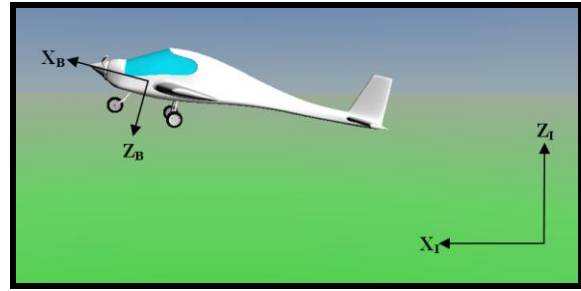


Figure 6: Simulation environment and three-dimensional model.

The solution of the governing equations was fed into the simulation environment instantaneously to simulate the airplane motion. The simulation started with the aircraft at rest on the runway, full thrust was applied and at a speed equal to  $1.1V_{stall}$  the airplane was rotated to start climbing. It was observed that the simulation results, based on the designed aircraft parameters, were in full agreement with the design goals; for example, the ground roll was less than 300 m and the rate of climb was about 3 m/s. In general, the simulation results illustrated the design ability to meet the design requirements.

### 4. Wing Stress Analysis and Design

Structural analysis of the airplane wing is conducted to define the geometry of the wing spars and skin. The wing section is designed to have two spars, one at a quarter of the chord position and one at the three quarters of the chord. Angled spar flanges are used along with stringers to stiffen the skin. It is assumed that the stringers and spar flanges only carry the direct normal stresses while the skin and spar webs carry the shear stresses; this enables the idealization of the stringers and flanges areas into a concentrated area named booms to carry the direct normal stresses along with the thin skin to carry the shear stresses. Proper stress analysis is used to calculate the area of the booms and the thickness of the skin. The finite element software COMSOL is utilized to verify the results of the structural analysis by employing the finite element method to calculate the stresses in the wing due to the aerodynamic loading. A wing-local coordinate system shown in figure 7 is adopted for the structural analysis.

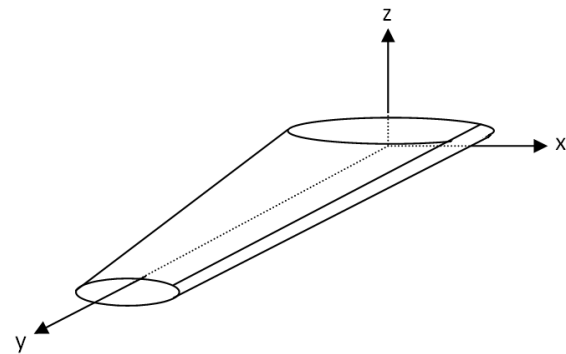


Figure 7: Wing-local coordinate system.

#### 4.1. Aerodynamic loads and pitching moment:

The aerodynamic forces that affect aircraft wings are the lift and drag. In the present study the lifting line theory is applied to achieve the span wise load distributions on the wing. A code written in MATLAB is developed in order to generate the span-wise load distribution.

First the unknown vortex strength distribution is approximated by the following Fourier series expansion [5]:

$$\Gamma(\beta) = 2bV_{\infty} \sum_{n=1}^N A_n \sin(n\beta) \quad (18)$$

Where

$$\beta = \cos^{-1} \left( -\frac{2y}{b} \right) \quad (19)$$

and y is the location of any airfoil section along the span. In order to determine the Fourier coefficients  $A_n$ , the following lifting line equation is solved [5],

$$\frac{4b}{a(y)c(y)} \sum_{n=1}^N A_n \sin(n\beta) + \sum_{n=1}^N nA_n \frac{\sin(n\beta)}{\sin(\beta)} = \alpha_G(y) - \alpha_o(y) \quad (20)$$

By obtaining the Fourier coefficients, the airfoil lift coefficient at any span-wise location is calculated using the following equation:

$$c_l = \frac{(4b \times A_n \sin((2K-1)\beta))}{c(y)} \quad (21)$$

where K in the above equation is the number of sections along the wing considered in the analysis, and  $c(y)$  is the chord length at different sections and is shown in the following equation:

$$c(y) = c_r \left( 1 - 2 \frac{\lambda-1}{b} y \right) = \frac{c_t}{\lambda} \left( 1 - 2 \frac{\lambda-1}{b} y \right) \quad (22)$$

The drag coefficient is calculated from the drag polar equation.

$$c_d = c_{d_o} + kc_l^2 \quad (23)$$

The lift and drag forces are calculated at each span wise location by using equations 24 and 25. The lift and drag distributions along the span are shown in figures 8 and 9.

$$L' = \frac{1}{2} \rho V_{\infty}^2 c c_l \quad (24)$$

$$D' = \frac{1}{2} \rho V_{\infty}^2 c c_d \quad (25)$$

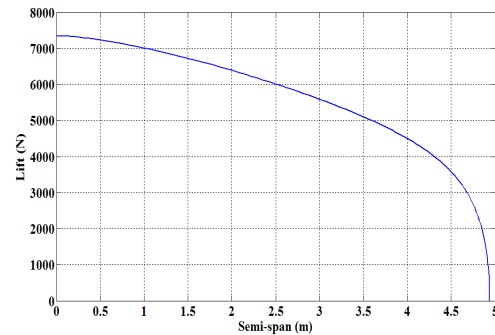


Figure 8: Lift distribution along the semi-span.

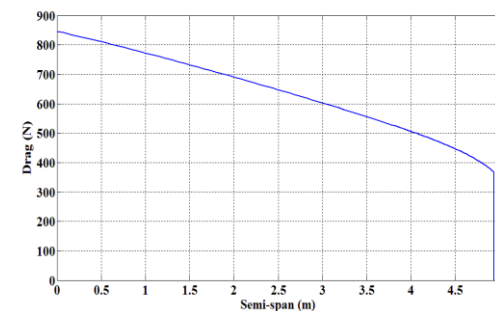


Figure 9: Drag distribution along the semi-span.

The pitching moment at each span-wise location is calculated by using the pitching moment coefficient and equation (26).

$$M = \frac{1}{2} \rho V_{\infty}^2 c^2 c_m \quad (26)$$

#### 4.2. Shear force and bending moment distributions:

The presence of the lift and drag forces create two shear forces,  $S_x$  and  $S_z$  along with two bending moments,  $M_x$  and  $M_z$ . As shown in the section of the aerodynamic analysis the wing was divided into finite segments to obtain the aerodynamic forces, lift and drag. The corresponding shear forces are calculated by multiplying the force by the segment on which it is acting. The bending moments on the wing are calculated from the shear forces. The span-wise distribution of the shear forces and the moments are shown in figures 10-13.

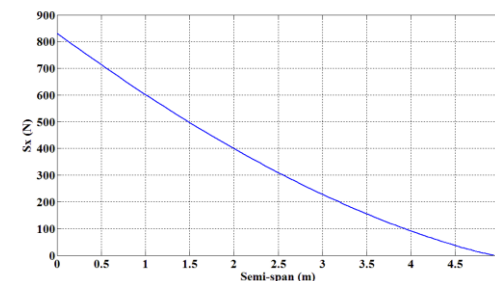


Figure 10: X-component shear stress distribution along the semi-span.

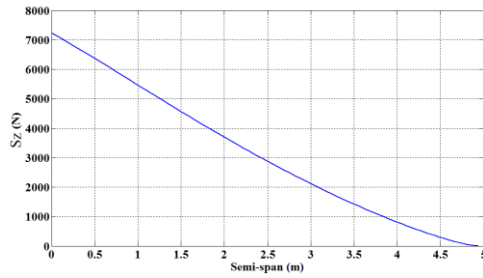


Figure 11: Z-component shear stress distribution along the semi-span.

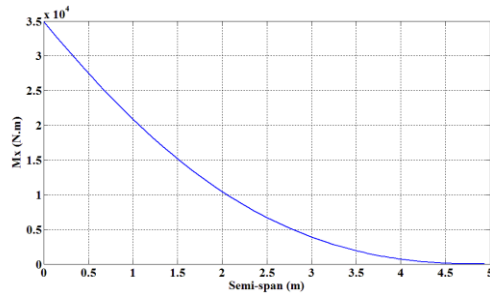


Figure 12: X-component bending moment distribution along the semi-span.

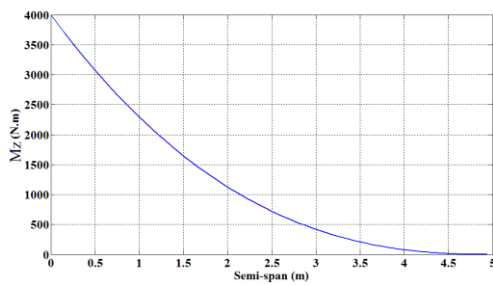


Figure 13: Z-component bending moment distribution along the semi-span.

4.3. Wing stress analysis:

As shown in figure 14, two idealized booms are placed at the quarter of the chord each having an area of  $A_b$ , and another two at three quarters of the chord each having an area of  $0.8A_b$ . The reason for a greater area at the quarter chord is due to the fact that the aerodynamic center is at that location requiring a larger area at that position. The following analysis calculates the area of the booms based on the bending stress analysis, and the thickness of the skin based on the shear flow in it, all at the root airfoil at which the loads are maximum.

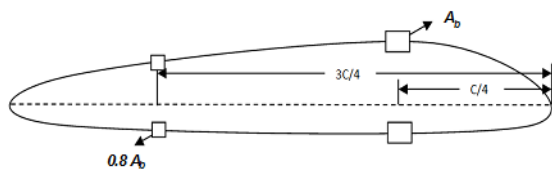


Figure 14: Schematic illustration of idealized booms and their location.

4.3.1. Boom area calculation:

The direct bending stresses are considered in the analysis to calculate the boom areas since the flanges of

the spars and the stringers are the areas that carry the bending stresses. First the centroid location is found in order to calculate the second moments of area of the booms. Using equations (27-29), the areas of the booms, which are imbedded in the second moment of area, are calculated by substituting the yield strength of the annealed steel 4140 alloy, with a factor of safety of 1.25, into equation (27). The area,  $A_b$ , was found to be  $0.0026 \text{ m}^2$ .

$$\sigma_y = \frac{\bar{M}_x}{I_{xx}} z + \frac{\bar{M}_z}{I_{zz}} x \tag{27}$$

$$\frac{\bar{M}_x}{I_{xx}} = \frac{M_x I_{zz} - M_z I_{xz}}{I_{xx} I_{zz} - I_{xz}^2} \tag{28}$$

$$\frac{\bar{M}_z}{I_{zz}} = \frac{M_z I_{xx} - M_x I_{xz}}{I_{xx} I_{zz} - I_{xz}^2} \tag{29}$$

In equation (27), (x and z) represent the location of the boom areas with respect to the pre-determined location of the centroid of the airfoil.

4.3.2. Skin thickness calculation:

Calculating the skin thickness was done by determining the shear flow in it by utilizing the shear forces acting on the wing. The shear center was first determined by substituting a value of zero for  $S_x$  then for  $S_z$  in equations (30) and (31). The shear forces are assumed to act at the shear center of the span-wise sections of the wing [11].

$$\frac{\bar{S}_x}{I_z} = \frac{S_x I_{xx} - S_z I_{xz}}{I_{xx} I_{zz} - I_{xz}^2} \tag{30}$$

$$\frac{\bar{S}_z}{I_{xx}} = \frac{S_z I_{zz} - S_x I_{xz}}{I_{xx} I_{zz} - I_{xz}^2} \tag{31}$$

The shear flow is then calculated by using equation (32):

$$q = q_b + q_{s,o} \tag{32}$$

In which q is the total shear flow in a closed section,  $q_b$  is the basic shear flow of an equivalent open section with  $q_{s,o}$  compensating for creating the open section. The open section is considered in order to simplify the determination of the shear flow. Having two spars in the wing creates a three-cell structure requiring three open sections. Accordingly, the shear flow of the open section  $q_b$  is calculated using equation (33).

$$q_b = - \left( \frac{S_x I_{xx} - S_z I_{xz}}{I_{xx} I_{zz} - I_{xz}^2} \right) \int_0^s t x ds - \left( \frac{S_z I_{zz} - S_x I_{xz}}{I_{xx} I_{zz} - I_{xz}^2} \right) \int_0^s t z ds \tag{33}$$

In which x and z are the coordinates within an airfoil section and s is the distance measured around the cross section. The value of  $q_{s,o}$ , which compensates for the cut in the closed structure, is calculated using equation (34) in

which  $G$  is the modulus of rigidity;  $A_c$  is the area of each cell and  $d\psi/dy$  is the gradient of twist.

$$\frac{d\psi}{dy} = \frac{1}{2A_c} \int \frac{q_{s,o}}{Gt} ds \tag{34}$$

The three-cell structure requires three cuts, which produces three versions of equation 34. The value of  $q_{s,o}$  for each cell is found by setting the rate of twist to zero at the shear center and solving the three equations simultaneously. The shear center is found by equating the summation of moments due to shear forces about the shear center to that produced from the shear flow. By determining the position of the shear center, the aero-loads are then applied at the aerodynamic center causing a rate of twist. The rate of twist for cells one and two form one equation and the rate of twist for cells two and three form another. Both equations have three variables  $q_1$ ,  $q_2$  and  $q_3$  which are the shear flows of the three cells. Therefore, a third equation is required. Here, the relationship between the external torque generated by the lift and drag forces along with the pitching moment on the shear center and the shear flow can be used and is shown below [11],

$$T = \sum_{i=1}^3 2A_{ci}q_i \tag{35}$$

Having the shear flow, the thickness of the skin of the wing can be computed by using equation (36) in which  $\tau$  is the shear strength of the skin material. The thickness was found to be 0.5 mm.

$$q = t \times \tau \tag{36}$$

**5. Finite Element Implementation**

In order to examine the designed wing and study its reliability, the commercial finite element software

COMSOL was used in order to model and analyze the wing under the calculated aerodynamic loads. The aerodynamic loads are defined as load per unit area over the upper surface boundaries. The boundary condition was fixed at the root of the wing while the whole model is meshed as shown in figure 15. In order to verify that the proposed design is safe and reliable, the distortion energy theory was applied to ensure that Von Mises stress divided by a factor of safety of 1.25 does not exceed the yield strength of the material used in the wing structure [12]. The FE model for the wing is constructed of two steel spar flanges with square cross sections; the spar flanges do not show explicitly in the geometry because they are defined as beams on the edges of the spar webs. The skin is defined as a shell along with the spar webs. Based on the results of the analysis, it was found that the maximum Von Mises stress was 681 MPa. By comparing the obtained Von Mises stress divided by the factor of safety with the yield strength of steel AISI 4140 (655 MPa) [12], it can be stated that the designed wing can sustain the loads according to the distortion energy theory. Figure 16 shows the Von Mises stress distribution in the wing structure. A maximum deflection of 9.1 cm in the out of plane direction is inflicted on the wing due to the load as shown in figure 17.

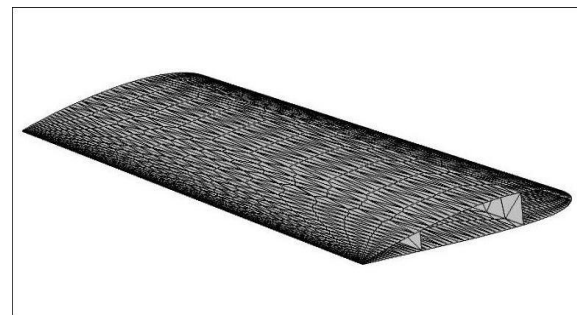


Figure 15: Wing model meshed using COMSOL commercial software.

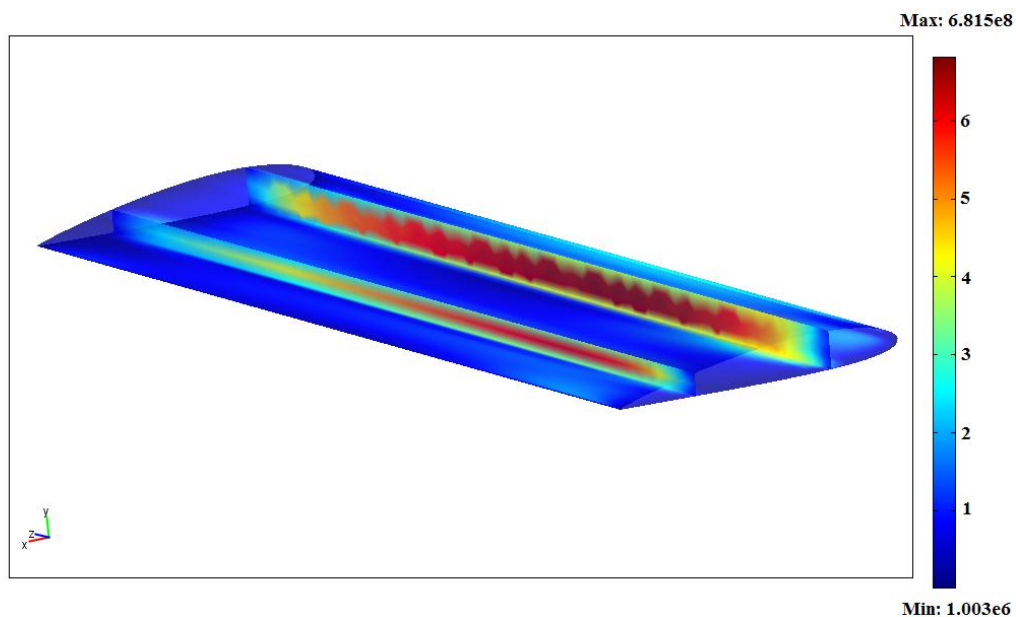


Figure 16: Von Mises stress distribution (Pa).



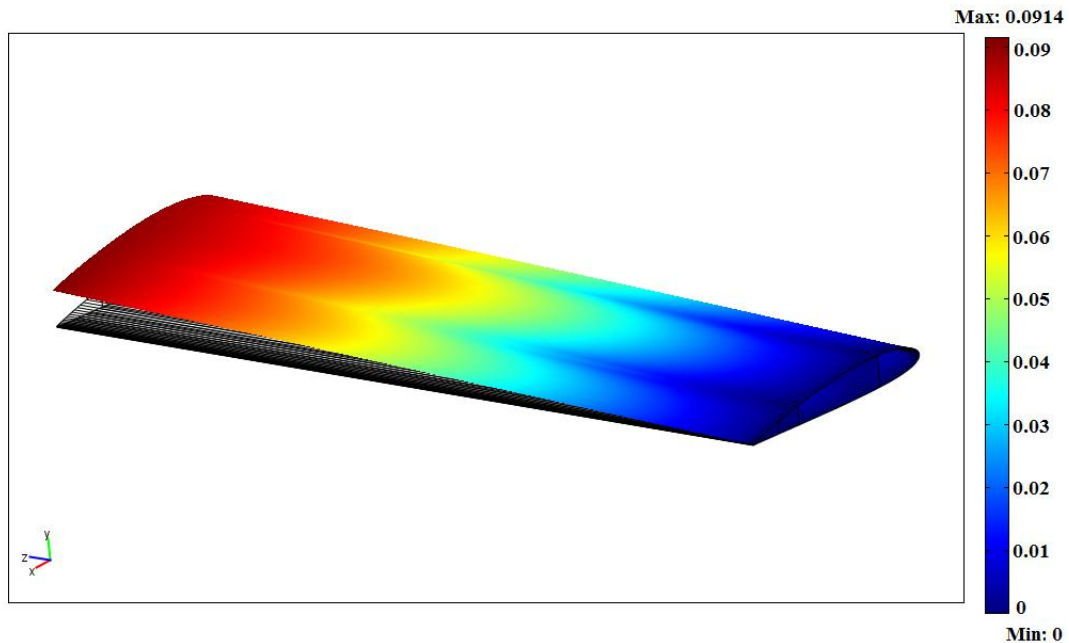


Figure 17: Wing deflection (m).

## 6. Conclusions

Conceptual design analysis of a general aviation aircraft was performed to estimate the gross take-off weight, the empty weight, the fuel weight and to size the major components of the aircraft based on a predefined set of design requirements. A design lay-out of the aircraft was also introduced by using conic lofting-based software. Subsequently, a simulation environment was created by using the Matlab Simulink to examine the performance of the designed aircraft during the take-off, climb, and cruise segments of the mission profile. The simulation has shown the adherence of the designed aircraft to the design requirements. The aerodynamic loads exerting on the

wings and the resulting span-wise shear force and bending moment distributions were obtained. Structural analysis was performed on the selected wings to calculate the boom areas of the spars and the thickness of the skin that enable the wings to withstand the generated aerodynamic forces and moments. To examine the structural effectiveness of the designed wing, 3-D finite element analysis was performed using COMSOL metaphysics software to model the wings, to compute the critical stresses and to test the wings against Von Mises failure criterion. Based on the finite element results, it was found that the designed wing is a safe candidate for the airplane to perform its mission and to meet all the design requirements.

## References

- [1] Gary L. Giles, "Design -oriented analysis of aircraft fuselage structures", NASA technical document, AIAA-98-1749, 1998
- [2] Saha, U.K., Mitra, M., Menon, S.J., John, N.T., Gajapathi, S.S., Behera, P., "Preliminary design analysis of a lightweight combat aircraft", Proceedings of the Institution of Mechanical Engineers, Part G, Journal of Aerospace Engineering, Vol. 222, No. 4, pp. 507-513, 2008.
- [3] E. Kessler and W.J. Vankan, "Multidisciplinary design analysis and multi-objective optimization applied to aircraft wing", National Aerospace Laboratory document, Netherland, 2006.
- [4] Mehdi Tarkian and Francisco J. Zaldivar Tessier, "Aircraft parametric 3D modeling and panel code analysis for conceptual design", 26<sup>th</sup> International Congress of the Aeronautical Sciences, Alaska, USA, 2008.
- [5] F., Al-Mawahra, O., Zaza, "Structural Analysis of an Aircraft Wing," Thesis submitted to the faculty of engineering, Jordan University of Science and Technology, June, 2009.
- [6] COMSOL Multiphysics, COMSOL Inc.
- [7] D.P., Raymer, Aircraft Design: A Conceptual Approach. American Institute of Aeronautics and Astronautics, Washington D.C, 1992.
- [8] V - Realm Builder, version 2.0, Integrated Data Systems Inc., 1996.
- [9] MATLAB, version 7.10.0.499 (R2010a), The MathWorks Inc., 2010.
- [10] J.D., Anderson, Jr., Aircraft Performance and Design. McGraw-Hill, 1999.
- [11] T.H.G., Megson, Aircraft Structures for Engineering Students", Elsevier Ltd, 2007.
- [12] R.G., Budynas, J.K., Nisbett, Shigley's Mechanical Engineering Design, McGraw-Hill, 2008.